Journal of Physiology (1990), **423**, *pp.* 193–220
With 9 figures
Printed in Great Britain

INTRABURST KINETIC PROPERTIES OF THE $GABA_A$ RECEPTOR MAIN CONDUCTANCE STATE OF MOUSE SPINAL CORD NEURONES IN CULTURE

BY ROY E. TWYMAN*, CARL J. ROGERS*
AND ROBERT L. MACDONALD*†

*From the Departments of *Neurology and †Physiology, University of Michigan Medical Center, Ann Arbor, MI 48104, USA*

(*Received 23 January 1989*)

SUMMARY

1. The intraburst kinetic properties of the main conductance state of γ-aminobutyric $acid_A$ ($GABA_A$) receptor channels in excised outside-out patches obtained from somata of mouse spinal cord neurones in cell culture were investigated using the patch clamp single-channel recording technique.

2. At 2 μM-GABA, the burst duration distribution was fitted by four exponential functions with time constants of 0·5, 2·4, 8·3 and 31·8 ms.

3. At 0·5, 1 and 2 μM-GABA, frequency distribution histograms of the number of apparent openings per burst were best fitted by three geometric functions with similar mean numbers (1·1, 1·9 and 3·6) of openings per burst. The proportion of bursts with a mean of 1·1 openings per burst decreased with increased GABA concentration while the proportion of bursts with means of 1·9 and 3·6 openings per burst increased with GABA concentration.

4. Analyses of GABA receptor channel intraburst kinetics were performed at all three GABA concentrations. The results were similar for all concentrations, but detailed results are presented only for 2 μM-GABA.

5. The open time distribution for all intraburst openings was best fitted by three exponential functions with time constants of 0·6, 2·9 and 8·9 ms.

6. Intraburst open time and total open time distributions for bursts with one to five openings were fitted with two or three exponential functions or gamma distributions, respectively. The number of components, time constants and relative areas were similar for both distributions.

7. The distributions of open times for the nth opening within bursts of k openings were similar for bursts containing two to five openings. The distributions of open times for the nth opening of all bursts varied with position within the burst. The distributions shifted to longer openings as the opening number increased from one to five.

8. The distributions of all closings within all bursts or within bursts with two to five openings and of closings relative to position in all bursts could be fitted by two exponential functions with time constants of about 0·20 and 3·1 ms and relative proportions of 0·55 and 0·45 at all GABA concentrations.

MS 7470

9. The total closed time distributions for bursts containing two to four closings, however, were all best fitted with only a single gamma distribution with a time constant of 1·3 ms.

10. These results suggest that the GABA receptor main conductance channel opens into at least one brief open state (O_1) from a singly liganded closed state and into at least two longer duration open states (O_2 and O_3) from doubly liganded closed states. Channel openings are grouped into bursts formed primarily by repeated openings of individual open states with the O_1, O_2 and O_3 states opening an average of 1·1, 1·9 and 3·6 times per burst, respectively. The brief intraburst closures may represent open channel blocked states or channel closed states which are independent of ligand-associated channel gating. A kinetic model is presented that is consistent with these observations.

INTRODUCTION

The main conductance state of the γ-aminobutyric $acid_A$ ($GABA_A$) receptor channel has been shown to open as single isolated openings and in bursts of openings (Hamill, Bormann & Sakmann, 1983; Sakmann, Hamill & Bormann, 1983; Bormann & Clapham, 1985; Martin, 1985; Bormann, Hamill & Sakmann, 1987; Weiss, Barnes & Hablitz, 1988; Macdonald, Rogers & Twyman, 1989). Nicotinic cholinergic (Dionne & Liebowitz, 1982; Labarca, Rice, Fredkin & Montal, 1985; Colquhoun & Sakmann, 1985; Sine & Steinbach, 1986; Hestrin, Korenbrot & Maricq, 1987; Jackson, 1988; Colquhoun & Ogden, 1988; Papke, Millhauser, Lieberman & Oswald, 1988), glycine (Hamill *et al.* 1983; Sakmann *et al.* 1983) and glutamate (Kerry, Kits, Ramsey, Sansom & Usherwood, 1987; Dudel & Franke, 1987; Kerry, Ramsey, Sansom & Usherwood, 1988; Howe, Colquhoun & Cull-Candy, 1988) receptor channels have been demonstrated also to open in complex bursts, suggesting similar gating properties among receptor-operated channels.

Bursting behaviour of receptor channels would be predicted if agonist binding and channel gating represented separate kinetic processes and if the channel opening rate was similar to the rate of agonist dissociation (del Castillo & Katz, 1957; Colquhoun & Hawkes, 1981). For the nicotinic cholinergic receptor, the following kinetic reaction scheme has been proposed.

$$2A + C_0 \underset{k_{-1}}{\overset{k_{+1}}{\rightleftharpoons}} A + AC_1 \underset{k_{-2}}{\overset{k_{+2}}{\rightleftharpoons}} 2AC_2 \underset{\alpha}{\overset{\beta}{\rightleftharpoons}} 2AO \qquad \text{Scheme (1)}$$

In scheme (1), A represents an agonist molecule, C_i represents the ith closed state, O represents an open state and the microscopic rate constants are as indicated. In such a scheme, the channel would open several times prior to agonist dissociation, producing bursts averaging two or more openings only if the agonist dissociation rate (k_{-2}) was equal to or less than the channel opening rate (β). The same scheme has been proposed for the GABA receptor (Bormann & Clapham, 1985).

Colquhoun & Sakmann (1985) investigated the intraburst kinetics of nicotinic receptors in adult frog muscle fibres and concluded that a more complex scheme (scheme (2)) was required. Scheme (2) is based on the work of del Castillo & Katz (1957), Monod, Wyman & Changeux (1965) and Karlin (1967).

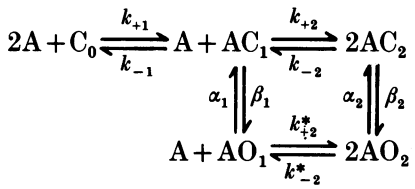

Scheme (2)

In scheme (2), O_i represents the ith open state. This scheme has also been proposed by a number of investigators (Colquhoun, 1973; Dreyer, Peper & Sterz, 1978; Dionne, Steinbach & Stevens, 1978; Colquhoun & Hawkes, 1982). The scheme has been used to explain the presence of two exponential components in open time frequency histograms and the presence of brief isolated openings and bursts of openings, which are thought to originate from the singly and doubly liganded receptors, respectively. Similarly, the gating properties of the GABA receptor have been modelled using scheme (2) (Bormann, 1988).

We have shown also that gating of the GABA receptor main conductance state of mouse spinal cord neurones in cell culture may be more complex than predicted by scheme (1) or by scheme (2) (Macdonald *et al.* 1989). We reported the presence of three exponential components in the open time frequency histogram and in the burst duration frequency histogram. To include these observations, we proposed a kinetic scheme (scheme (3)) which is a modification of scheme (2). In scheme (3) the singly bound receptor opens into a single brief open state to produce primarily single openings and the doubly bound receptor opens into two longer duration open states to produce bursts of openings.

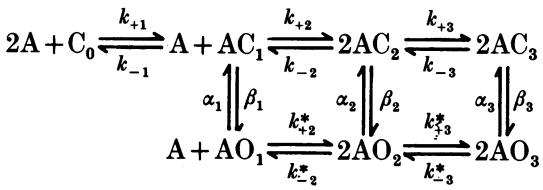

Scheme (3)

This kinetic model is testable. We have now studied the intraburst kinetics of the main conductance state of the GABA receptor channel to determine if the gating properties of the GABA receptor channel recorded from outside-out patches obtained from mouse spinal cord neurones in cell culture are consistent with the kinetic model in scheme (3).

METHODS

Cell culture

Spinal cords were dissected from 12- to 14-day-old murine fetuses and grown in cell culture as described previously (Ransom, Neale, Henkart, Bullock & Nelson, 1977; Macdonald *et al.* 1989). Cultures were maintained for 2–5 weeks prior to being used in these experiments.

Solutions and GABA application

All drugs were obtained from Sigma Chemical Co. (St Louis, MO, USA). The medium used to grow and maintain the cultures was exchanged for 2 ml of extracellular salt solution which consisted of the following (in mM): 142 NaCl, 8·1 KCl, 1 $CaCl_2$, 6 $MgCl_2$, 10 glucose, 10 Na-HEPES

(pH 7·4). To ensure that glycine-activated chloride current did not contaminate the recordings, the specific glycine receptor antagonist strychnine (200 nM) was added to the extracellular solution at a concentration that did not alter GABA responses. The intrapipette solution contained (in mM): 153 KCl, 1 $MgCl_2$, 10 K-HEPES, 5 EGTA, 1 NaOH, 2 KOH (pH 7·38). This combination of extracellular and intrapipette solutions resulted in a chloride equilibrium potential (E_{Cl}) of about 0 mV and a potassium equilibrium potential (E_K) of −75 mV across the patch membrane. All experiments were performed at room temperature (20–23 °C).

GABA was diluted with extracellular solution from a 1 mM stock solution to a final concentration of 0·5, 1 and 2 μM on the day of the experiment. GABA was applied to the patch membrane for 20 s via pressure ejection micropipettes which were moved to within 50 μm of patches only during the time of GABA application.

Current recording techniques

Recording techniques were similar to those previously described (Hamill, Marty, Neher, Sakmann & Sigworth, 1981; Macdonald *et al.* 1989). Excised outside-out patches were obtained using a model L/M EPC-7 amplifier (LIST-Medical Instruments, Darmstadt, FRG) and were simultaneously recorded on a video cassette recording system (VCR; SONY SL-2700) via a digital audio processor (SONY PCM-501 ES, modified to 0–20 kHz, 14-bit resolution, 44 kHz sampling frequency) and a chart recorder (Gould Inc., Cleveland, OH, USA). At a later time, the data were played back from the VCR and digitized (8 kHz, 14 bit) with a 1 kHz (3 dB) 8-pole Bessel filter (Frequency Devices, Haverhill, MA, USA) interposed. Current amplitudes and durations were determined by computer using software previously described (Macdonald *et al.* 1989). Openings and closings were detected using the 50 % threshold crossing method and were accepted as valid events if their durations were greater than twice the system dead time (dead time = 170 μs). Measured open and closed times will generally be longer than 'true' open and closed times due to undetected closings and openings. Throughout the text the terms 'open and closed times' will refer to measured times that have not been corrected for unobserved transitions (McManus, Blatz & Magleby, 1987).

Definition of bursts and evaluation of events per burst

Bursts may be defined as openings or groups of openings separated by relatively long closed periods (Colquhoun & Sigworth, 1983). For the purpose of this analysis, a critical closed time or burst terminator, t_c, was chosen such that all openings separated by closures less than t_c belonged within a burst, and bursts were separated by closures greater than t_c. A modification of the equal proportion of misclassification method of Colquhoun & Sakmann (1985) was used to select a t_c of 5 ms which would result in misclassification of 2·4 % of the closures from the short and long closed time distributions (Macdonald *et al.* 1989).

The structure of bursts was defined as follows. A burst could contain 1 to k openings. Sequential openings from first to last opening within a burst were designated $n = 1, 2, \ldots, k$. Sequential closings after the first opening were designated $n = 1, 2, \ldots, k-1$. The bursts contained one fewer closing than openings.

The distribution of openings per burst may be fitted by the sum of one or more geometric functions using eqn (1) (Colquhoun & Hawkes, 1982, 1983). The number of components in the distribution provides a lower limit for the number of open states.

$$P(r) = \sum_{i=1}^{n} a_i \mu_i^{-1}(1-\mu_i^{-1})^{r-1}. \quad (1)$$

In eqn (1), $P(r)$ is the probability of r apparent openings per burst, a_i is the relative proportion of the ith component ($a_1 + a_2 + \ldots + a_n = 1$) and μ_i is the mean number of openings of the ith component.

Analysis of open and closed time frequency histograms

Open and closed times were placed in time bins and plotted in appropriate frequency histograms to minimize bin promotion errors (McManus *et al.* 1987). Frequency histograms of open or closed durations were fitted to a sum of exponentials using eqn (2).

$$f(t) = \sum_{i=1}^{n} a_i \exp(-t/\tau_i)/\tau_i. \quad (2)$$

In eqn (2), $f(t)$ is the probability density function for open or closed times containing n components, τ_i is the time constant of the ith component and a_i is the relative area of the ith component ($a_1+a_2+\ldots+a_n=1$). Time constants and relative areas are given with error ranges (see Statistics below).

Total open and closed time distributions

Intraburst total open and closed times were placed in time bins and plotted in appropriate frequency histograms. Frequency histograms of intraburst total open or closed durations were fitted to a sum of gamma distributions using eqn (3).

$$f_k(t)=\sum_{i=1}^{n} a_i(\tau_i^{-1})\,(t/\tau_i)^{k-1}\exp(-t/\tau_i)/(k-1)!. \quad (3)$$

In eqn (3), $f_k(t)$ is the probability density function for total open time within a burst of k openings containing n components, τ_i is the time constant of the ith open component and $a_1+a_2+\ldots+a_n=1$.

Statistics

The method of maximum likelihood was used for non-linear curve fitting of all frequency histograms (Colquhoun & Sigworth, 1983). Error ranges of components were determined by likelihood intervals ($m=2$ to approximate 95% confidence levels; Macdonald *et al.* 1989). Events per burst histograms were fitted from the first to twentieth bin. Event duration histograms were fitted from bins starting from at least twice the system dead time. The number of geometric, exponential or gamma components present in a distribution was determined by χ^2 analysis such that the estimated fit and data were within the 95% confidence interval for accepting the null hypothesis (no difference between data and fit). Means are presented mean ± S.D. unless otherwise indicated.

RESULTS

Burst durations

Prior to application of GABA, rare, brief, spontaneous inward currents were seen. GABA (2 μM) evoked isolated openings which appeared to be brief (Fig. 1*A*, single asterisk) and bursts of openings which appeared to be more complex (Fig. 1*A*, double asterisks). At higher temporal resolution, the bursts appeared to differ in duration and complexity (Fig. 1*B–D*). Openings occurred in short bursts composed of relatively brief openings (Fig. 1*D*, single asterisk) and in longer bursts composed of relatively longer openings (Fig. 1*D*, double asterisks).

The presence of multiple burst components evoked by GABA (2 μM) was also apparent in the burst duration frequency distribution which was fitted significantly by the sum of three exponential functions with time constants of 0·65, 5·5 and 28·9 ms and relative areas of 0·31, 0·42 and 0·27 (Fig. 1). In principle, however, the number of exponential components required to fit the burst duration frequency histogram should be larger than the number of open states (Colquhoun & Hawkes, 1982). Since we have proposed that three open states are present, a four-exponential fit was obtained with time constants of 0·54, 2·4, 8·3 and 31·8 ms and relative areas of 0·26, 0·19, 0·33 and 0·22 which resulted in an improved χ^2 value.

Openings per burst

There was a concentration-dependent increase in the mean number of apparent openings per burst (Fig. 2, insets). The mean number of openings per burst was 1·4 in 0·5 μM-GABA, 1·6 in 1 μM-GABA, and 1·9 in 2 μM-GABA. With increasing GABA

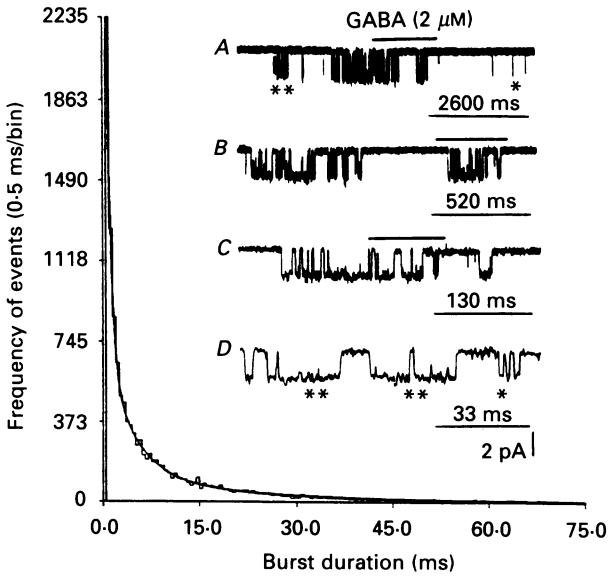

Fig. 1. GABA (2 μM)-evoked bursting inward single-channel currents. Currents are shown at increasing time resolution in the inset (*A–D*). Burst durations were binned into 0·5 ms bins and displayed over a range of 1–75 ms. The portion of the current record under the thick horizontal line above each trace is presented expanded in time in the tracing below it. Openings occurred in isolation (*A*, *) or in groups of openings (*A*, **). At higher time resolution, openings of relatively shorter duration (*D*, *) and openings of relatively longer duration (*D*, **) appeared to occur together in separate groups. Time calibration for each trace is shown on the right below the trace. Current calibration at lower right applies throughout. The plot is the frequency distribution of GABA (2 μM)-evoked burst durations. The distribution was fitted to the sum of three exponential functions. The histogram contains 15560 bursts. See the text for further details.

concentration, the normalized openings per burst frequency histograms were shifted to greater numbers of openings per burst (Fig. 2*A–C*).

The openings per burst frequency histograms at each GABA concentration (Fig. 2) were best fitted with three geometric functions (see Methods) with different mean numbers of openings per burst. The estimated mean numbers of openings per burst for each component were concentration-independent (Table 1). The geometric components were composed of an average number of events per burst (mean ± S.D.) of 1·07 ± 0·04, 1·9 ± 0·4 and 3·6 ± 0·3 openings per burst. The relative area of the burst component with the fewest number of openings per burst declined with increasing GABA concentration while the relative areas of the two components with more openings per burst increased with increasing GABA concentration.

Thus, bursts occurred with three concentration-independent mean numbers of openings and openings occurred with three concentration-independent time constants. The relationships among these complex bursts and openings can be determined only by a more detailed analysis of intraburst open and closed state kinetics (Colquhoun & Hawkes, 1982).

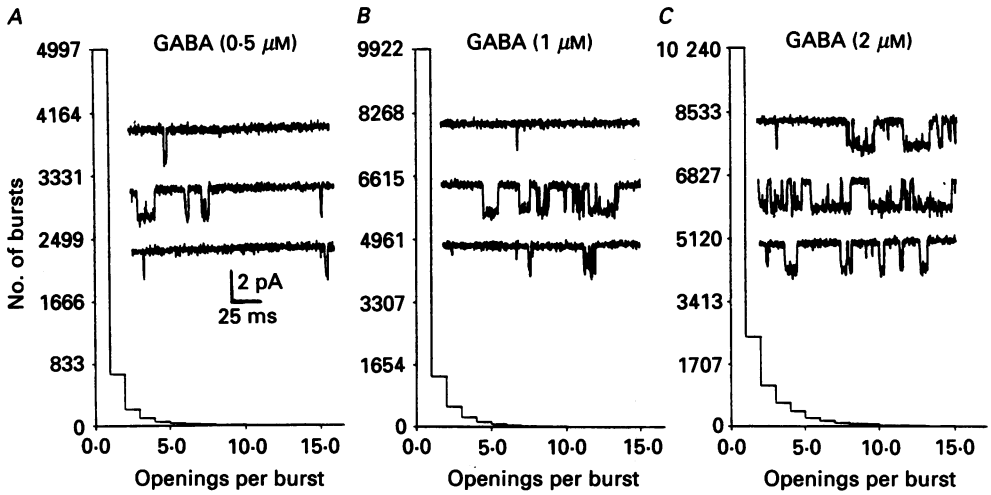

Fig. 2. Frequency distributions of the number of apparent openings per burst. The numbers of bursts are plotted against the numbers of detected openings per burst for 0·5 (*A*), 1, (*B*), and 2 μM (*C*) GABA. Histograms contain 6223 bursts for 0·5 μM, 12448 bursts for 1 μM and 15560 bursts for 2 μM-GABA. Raw data insets display short representative segments of GABA-evoked currents at each concentration. Calibration in *A* applies to each current trace.

TABLE 1. Openings per burst: components of geometric functions

[GABA]	0·5 μM	1·0 μM	2·0 μM
μ_1	1·07 (1·06–1·09)	1·03 (1·02–1·03)	1·11 (1·10–1·12)
μ_2	1·7 (1·7–1·9)	1·7 (1·6–1·7)	2·2 (ND)
μ_3	3·7 (2·8–5·1)	3·3 (3·0–3·5)	3·8 (3·5–4·1)
a_1	0·70 (ND)	0·60 (0·49–0·72)	0·50 (0·37–0·64)
a_2	0·23 (0·21–0·24)	0·30 (0·29–0·31)	0·35 (0·52–0·54)
a_3	0·08 (0·05–0·10)	0·10 (0·09–0·10)	0·15 (0·13–0·15)

The distributions of the number of apparent openings per burst were fitted with the sum of three geometric functions (using eqn (1)) for each concentration of GABA (0·5, 1 and 2 μM). See Fig. 2 for plots of the histograms. The geometric means μ_1, μ_2 and μ_3 are the means of components 1, 2 and 3, respectively, of the geometric functions. The corresponding relative areas of each component are a_1, a_2 and a_3, respectively. Error ranges as determined by likelihood analysis ($m = 2$) are in parentheses. ND, indeterminate ranges.

Intraburst open times in all bursts and in bursts with one to five openings

For GABA (2 μM), open durations for all openings (Fig. 3*A*) and for openings in one to five opening bursts (Fig. 3*B*) were collated into frequency histograms. The frequency distribution of all openings evoked by GABA (2 μM; Fig. 3*A*) was best fitted with three exponential functions with time constants of 0·59, 2·9 and 8·9 ms and relative areas of 0·17, 0·54 and 0·29, respectively.

For bursts with numbers of openings increasing from one to five ($k = 1$–5), there was an increase in the proportion of longer openings (Fig. 3*B*). The intraburst open time frequency histogram for bursts with one to five openings were fitted with multiple exponential functions. While the time constants of the exponential

functions fitted to the open time frequency histograms for bursts with one to five openings (Table 2) increased slightly with increasing numbers of openings per burst, they were not significantly different from those found for the three exponential functions fitted to the open time frequency histogram for all openings. The increase in time constant with increased numbers of openings per burst was probably due to increased numbers of missed brief closures (see Discussion). However, the relative

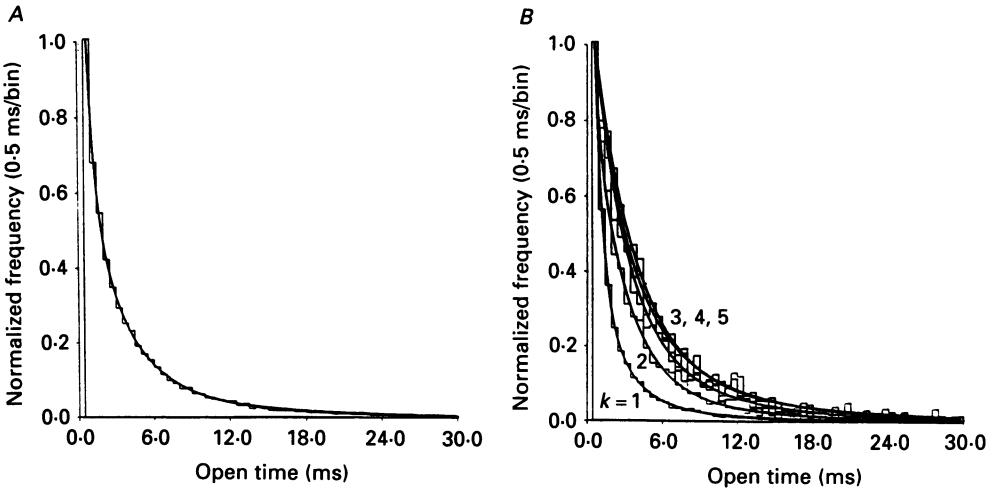

Fig. 3. Distribution of all openings in all bursts and in bursts containing one to five openings (2 μM-GABA). Open times were binned into 0·5 ms bins and displayed over a range of 1–30 ms. *A*, normalized frequency distribution of open time for all openings in all bursts (open time distribution of all detected openings). Histogram contains 29518 openings. The distribution was fitted with three exponential functions (see text). *B*, normalized frequency distributions of open time for all openings in bursts containing $k = 1$, 2, 3, 4 or 5 openings. Distributions were fitted with three exponential functions in the open time distributions for bursts containing only one ($k = 1$) or two ($k = 2$) openings. For bursts containing three, four or five openings ($k = 3$, 4 or 5, respectively), open time distributions were fitted with two exponential functions. Histograms contained 10240 openings for $k = 1$, 4032 openings for $k = 2$, 3381 openings for $k = 3$, 2288 openings for $k = 4$ and 2100 openings for $k = 5$ bursts.

areas of the three components were quite different for bursts with different numbers of openings (Table 2). The relative area of component one declined as the number of openings per burst increased from one to two. Component one could not be resolved in bursts with more than two openings. The relative area of component two increased as the number of openings per burst increased from one to two and decreased as the number of openings per burst increased from two to five. The relative area of component three increased as the number of openings per burst increased from one to five.

These results demonstrated that the distribution of open times in bursts containing one to five openings were best fitted with exponential functions with time constants similar to those obtained for the distribution of all openings and are consistent with the presence of three open states. In addition, these findings imply that the longer, more complex bursts (bursts with two or more openings) were composed of openings primarily to the two longer open states. Similar results were obtained for lower

TABLE 2. All openings in bursts with k openings: components of exponential functions

	$k = 1$	$k = 2$	$k = 3$	$k = 4$	$k = 5$
τ_1	0·56 (0·51–0·60)	0·3 (0·18–0·61)	—	—	—
τ_2	2·2 (2·0–2·3)	2·5 (2·3–2·8)	2·7 (2·4–3·0)	2·7 (2·4–3·2)	2·8 (2·4–3·4)
τ_3	7·5 (6·6–8·3)	8·9 (7·8–10·1)	8·8 (7·8–9·7)	8·4 (7·4–9·4)	9·5 (8·3–10·6)
a_1	0·40 (0·38–0·41)	0·09 (0·05–0·13)	—	—	—
a_2	0·44 (0·42–0·46)	0·65 (0·61–0·69)	0·64 (0·60–0·68)	0·54 (0·47–0·59)	0·52 (0·45–0·60)
a_3	0·16 (0·14–0·19)	0·26 (0·21–0·30)	0·36 (0·31–0·41)	0·46 (0·39–0·53)	0·48 (0·41–0·56)

The distributions of all openings in bursts with k openings (k = 1–5) were fitted with a sum of exponential functions (eqn (2)). Data were obtained using 2 μM-GABA. The values for τ_i and a_i for exponential components $i = 1, 2, 3$ and their error ranges as determined by maximum likelihood analysis ($m = 2$) are presented. Time constants are in milliseconds. Components designated by dashes indicate that those components were not found in the curve fitting.

TABLE 3. nth opening in all bursts: components of exponential functions

	$n = 1$	$n = 2$	$n = 3$	$n = 4$	$n = 5$
τ_1	0·56 (0·50–0·62)	—	—	—	—
τ_2	2·6 (2·5–2·7)	2·5 (2·3–2·7)	3·4 (3·0–3·8)	2·5 (2·1–3·0)	3·5 (2·7–4·5)
τ_3	8·7 (7·9–9·5)	9·1 (8·4–9·9)	10·2 (8·9–11·5)	8·3 (7·5–9·1)	8·4 (7·1–9·8)
a_1	0·32 (0·30–0·33)	—	—	—	—
a_2	0·50 (0·52–0·48)	0·67 (0·63–0·70)	0·53 (0·48–0·58)	0·51 (0·44–0·56)	0·56 (0·45–0·64)
a_3	0·18 (0·16–0·20)	0·33 (0·29–0·37)	0·47 (0·41–0·53)	0·49 (0·42–0·56)	0·44 (0·34–0·53)

The distributions of the nth opening in all bursts (n = 1–5) were fitted with a sum of exponential functions (eqn (2)). Data were obtained using 2 μM-GABA. The values for τ_i and a_i for exponential components $i = 1, 2, 3$ and their error ranges as determined by maximum likelihood analysis ($m = 2$) are presented. Time constants are in milliseconds. Components designated by dashes indicate that those components were not found in the curve fitting.

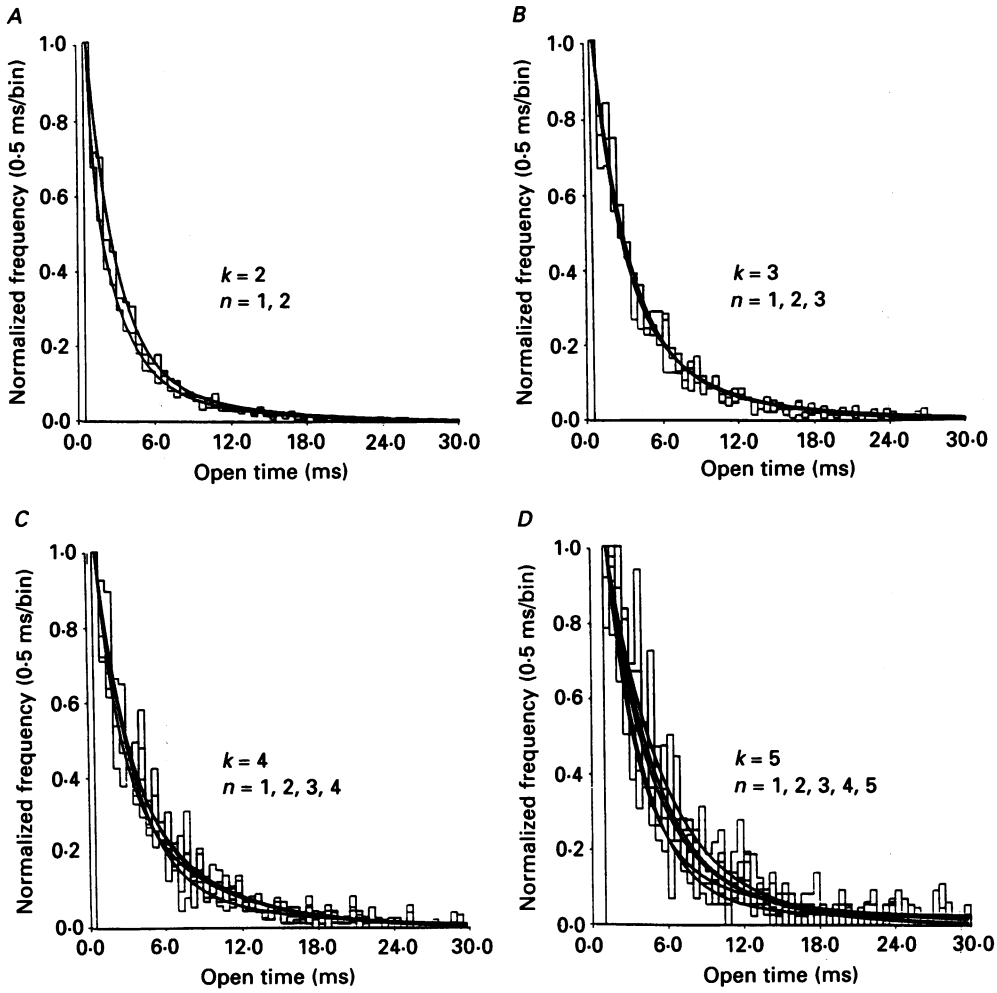

Fig. 4. Distribution of openings relative to position in bursts with one to five openings (2 μM-GABA). Openings were binned into 0·5 ms bins and displayed over a range of 1–30 ms. *A*, normalized frequency distributions of the first $n = 1$) and second ($n = 2$) openings of bursts containing two openings ($k = 2$). Distributions were fitted with three exponential functions. Each histogram contained 2466 openings. *B*, normalized frequency histograms of the first ($n = 1$), second ($n = 2$) and third ($n = 3$) openings of bursts containing three openings ($k = 3$). Distributions were fitted with two exponential functions. Each histogram contained 1127 openings. *C*, normalized frequency histograms of the first to fourth openings ($n = 1$, 2, 3 and 4) of bursts containing four openings ($k = 4$). Distributions were fitted with two exponential functions. Each histogram contained 647 openings. *D*, normalized frequency distribution of the first to fifth openings ($n = 1$, 2, 3, 4 and 5) of bursts containing five openings ($k = 5$). Distributions were fitted with two exponential functions. Each histogram contained 420 openings.

concentrations of GABA (0·5 and 1 μM) except that there was a larger proportion of the brief openings in the distribution of all openings and of bursts with one or two openings (not illustrated).

Open times with respect to position in one to five opening bursts

To further characterize the intraburst openings, open times may be examined with respect to their position within bursts (Colquhoun & Hawkes, 1982). With the assumption of microscopic reversibility, the open time probability density function from a particular open state should be symmetrical in time (Colquhoun & Hawkes, 1982). That is, the probability density function for open times occurring in the first position of a burst should be similar to that for open times occurring in the last

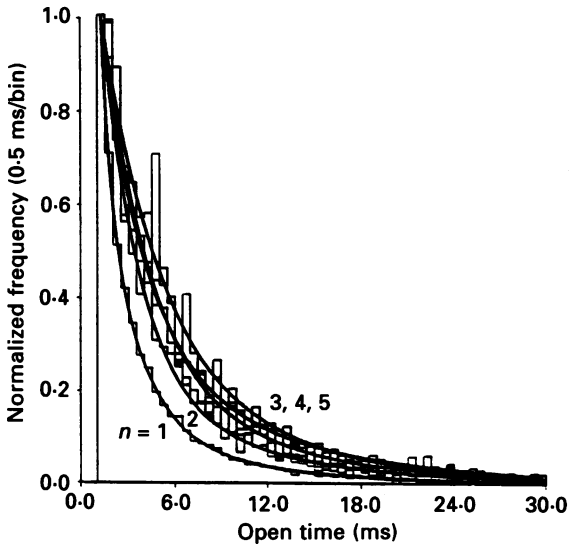

Fig. 5. Distributions of openings relative to position in all bursts (2 μM-GABA). Openings were binned in 0·5 ms bins and displayed over a range of 1–30 ms. The frequency distributions of the first ($n = 1$), second ($n = 2$), third ($n = 3$), fourth ($n = 4$) and fifth ($n = 5$) openings of all bursts are shown with corresponding curve fits. The distribution of the first and second openings were fitted with three exponential functions. The distributions of the third, fourth and fifth openings were fitted with two exponential functions. Histograms contained 15560, 5420, 2954, 1827 and 1180 openings for $n = 1$, 2, 3, 4 and 5 opening distributions, respectively.

position of a burst. Furthermore, the probability density function for open times occurring in the second position should be similar to those occurring in the second to last position in a burst. For 2 μM-GABA, the open time frequency histograms of openings in any position (n) in a burst of k openings overlapped for two ($k = 2$; $n = 1$, 2; Fig. 4*A*), three ($k = 3$; $n = 1$, 2, 3; Fig. 4*B*), four ($k = 4$; $n = 1$, 2, 3, 4; Fig. 4*C*) and five ($k = 5$; $n = 1$, 2, 3, 4, 5; Fig. 4*D*) opening bursts. Curve fitting of these histograms required the sum of two or three exponential functions that were similar for each opening position in each type of burst (Fig. 4*A–D*). The time constants and relative areas of the exponential functions for all openings in bursts with k openings were similar (numerical values not presented). In addition, the time constants were similar to those found in the analysis of histograms from all openings

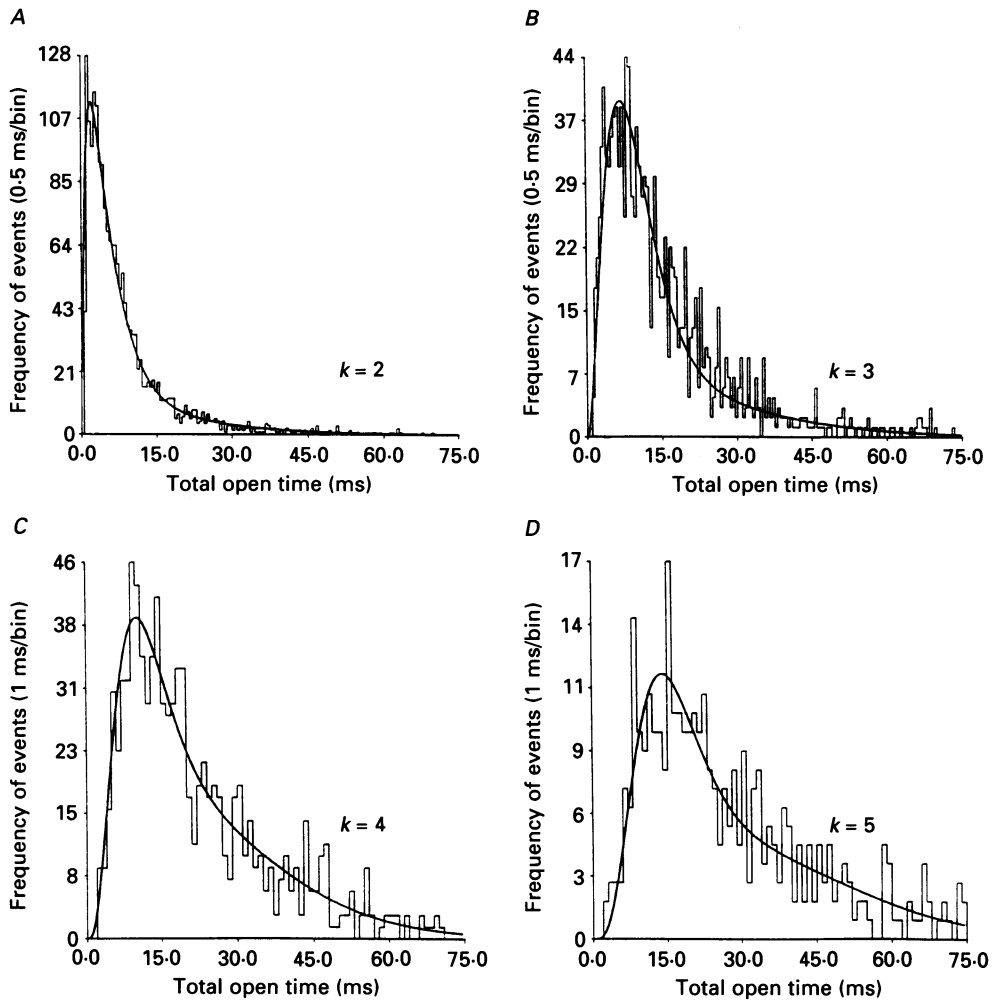

Fig. 6. Distributions of total open time within bursts containing two to five openings (2 μM-GABA). Total open durations in two ($k = 2$; *A*) and three ($k = 3$; *B*) opening bursts were binned in 0·5 ms bins and displayed over a range of 1–75 ms. For four ($k = 4$; *C*) and five ($k = 5$; *D*) opening bursts, total open durations were binned in 1·0 ms bins and displayed over a range of 1–75 ms. The distribution of total open time for two opening bursts (*A*) contained 2466 bursts and was fitted with a sum of three gamma distributions. The distributions for three (*B*), four (*C*) and five (*D*) opening bursts contained 1127, 647 and 420 bursts, respectively. Each was fitted with a sum of two gamma distributions.

of two, three, four and five opening bursts (Fig. 3*B*). Similar results were obtained for openings in bursts evoked by 0·5 and 1 μM-GABA (not illustrated).

Open times with respect to position in all bursts

Further evaluation of the distribution of openings within bursts was done by collating open times occurring in the first, second, third, fourth and fifth ($n = 1$–5) position in all bursts (Colquhoun & Hawkes, 1982). There was a shift in the frequency histograms to longer openings as the open position in any burst increased from the

TABLE 4. Total open time of k opening bursts: components of gamma distributions

	$k = 1$	$k = 2$	$k = 3$	$k = 4$	$k = 5$
τ_1	0·56 (0·51–0·60)	1·1 (0·8–1·6)	—	—	—
τ_2	2·2 (2·0–2·3)	3·0 (2·7–3·4)	3·3 (2·9–3·9)	3·3 (2·6–4·1)	3·4 (2·9–4·0)
τ_3	7·5 (6·6–8·3)	9·9 (8·6–11·1)	11·0 (9·6–12·9)	8·8 (7·9–9·9)	9·1 (8·1–10·1)
a_1	0·45 (0·43–0·46)	0·08 (0·06–0·12)	—	—	—
a_2	0·45 (0·43–0·47)	0·67 (0·59–0·75)	0·68 (0·57–0·80)	0·63 (0·42–0·84)	0·56 (0·42–0·71)
a_3	0·10 (0·08–0·13)	0·25 (0·18–0·30)	0·32 (0·27–0·36)	0·37 (0·29–0·44)	0·44 (0·35–0·52)

The distributions of total open time in bursts with k openings ($k = 1$–5) were fitted with a sum of gamma distributions (eqn (3)). Data were obtained using 2 μM-GABA. The values for τ_i and a_i for gamma distribution components $i = 1, 2, 3$ and their error ranges as determined by maximum likelihood ($m = 2$) are presented. Time constants are in milliseconds. Components designated by dashes indicate that those components were not found in the curve fitting.

first to the fifth position (Fig. 5). Curve fitting of these frequency histograms revealed time constants (Table 3) similar to those for the three exponential components obtained in the fit of the open time distribution of all openings (Fig. 3*A*). Time constants for the first opening were 0·56, 2·6 and 8·7 ms. Frequency histograms of the second, third, fourth and fifth opening of any burst were best fitted with only two exponential functions. The estimated time constants of the two components did not

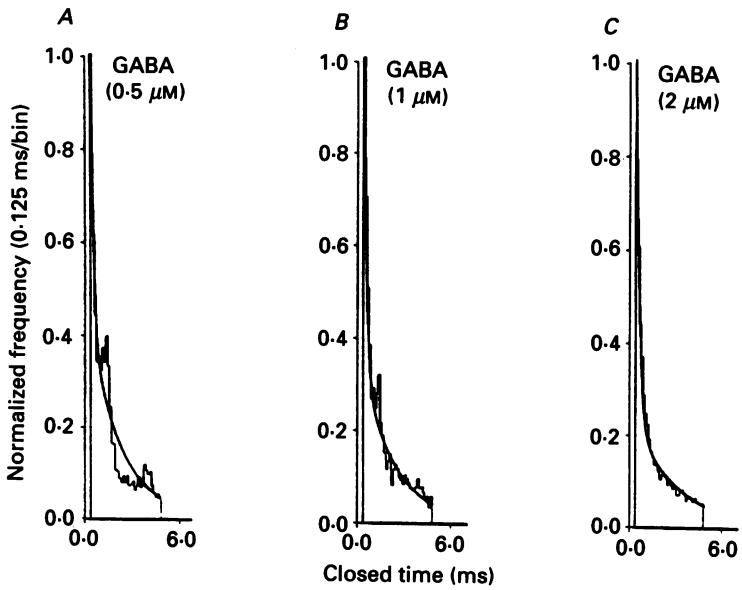

Fig. 7. Normalized frequency distributions of intraburst closings for all bursts evoked by 0·5, 1 and 2 μM-GABA. Closed times were binned in 0·125 ms bins and displayed over a range of 0·375–5·0 ms. Distributions were fitted with two exponential functions. Histograms contained 2897, 5541 and 13858 closings for 0·5, 1 and 2 μM-GABA, respectively.

vary, ranging from 2·5 to 3·5 ms and 8·3 to 10·2 ms. The time constants of the three components were similar to those of the three components of the open time distribution. The relative areas of the three components varied with the position of the opening in the bursts. The shortest component could only be resolved in the distribution of the first opening of all bursts. The relative area of the second component increased in the distribution of the second opening of all bursts and then declined in the distributions of the third to fifth opening in all bursts. The relative area of the third component increased progressively as the opening occurred later in a burst. Similar results were obtained for bursts evoked by 0·5 and 1 μM-GABA except that with the lower GABA concentrations there was a higher proportion of the brief (component one) openings.

Total open time per burst

The total open time frequency histogram of one opening bursts was best fitted with the sum of three exponential functions (Fig. 3*B*, Table 2). The same results were obtained using eqn (3) with $k = 1$. The total open time frequency histograms of bursts with two to five openings ($k = 2$–5) were best fitted with two or more gamma

distributions (Fig. 6). For 2 μM-GABA, the total open time histograms for two (Fig. 6*A*) opening bursts were best fitted with three gamma distributions and three (Fig. 6*B*), four (Fig. 6*C*) and five (Fig. 6*D*) opening bursts were best fitted with two gamma distributions. The time constants for the three total open time gamma distributions (Table 4) were similar to the time constants for the three overall open time and intraburst open time exponential functions (Tables 2 and 3).

The relative areas of the three components varied among bursts with different numbers of openings (Table 4). For 2 μM-GABA, the relative area of the first component was maximal in one opening bursts and declined to a minimal contribution for three or more opening bursts. The relative area of the second component increased to a maximum in two to three opening bursts and declined in three to five opening bursts. The relative area of the third component was minimal in the one opening bursts but increased progressively in bursts with increasing numbers of openings.

Similar time constants were found for the gamma distribution fits of k event burst total open time frequency histograms for 0·5 and 1 μM-GABA (not shown). The relative proportion of the component with the shortest time constant was greatest in 0·5 μM-GABA and declined as the concentration of GABA increased. The relative contribution of the two components with longer time constants increased as the number of openings per burst increased.

Intraburst closed times

Similar to the analysis presented above, the properties of intraburst closings can be characterized by analysing geometric and closed time distributions and intraburst closed time and total closed time distributions for two to five opening bursts. The distributions of observed intraburst closed times can be compared with those predicted by kinetic scheme (3).

We have reported previously that mean intraburst closed time was GABA concentration-independent and ranged from 1·5 to 1·6 ms (Macdonald *et al.* 1989). Consistent with this, intraburst closed time frequency histograms varied little with concentration (Fig. 7). The histograms were best fitted with two exponential functions. The time constants of the two functions were GABA concentration-independent and averaged $0{\cdot}17 \pm 0{\cdot}03$ and $2{\cdot}4 \pm 0{\cdot}5$ ms. The relative areas of the functions were also concentration-independent and averaged $0{\cdot}56 \pm 0{\cdot}03$ and $0{\cdot}44 \pm 0{\cdot}03$, respectively.

For 2 μM-GABA, intraburst closed time frequency histograms did not appear to vary significantly with the number of openings per burst (Fig. 8*A*). The frequency histograms were best fitted with two exponential functions. Increasing from two to five opening bursts, the shortest time constants were 0·24, 0·22, 0·21 and 0·18 ms while the longest time constants were 4·5, 3·1, 3·0 and 2·4 ms, respectively. While there was a trend for both the short and long time constants to decrease as the number of closings per burst increased, the 95% confidence intervals for the short or long time constants were overlapping. The time constants of the two components averaged $0{\cdot}21 \pm 0{\cdot}02$ and $3{\cdot}2 \pm 0{\cdot}9$ ms. The trend for decreasing time constants with increasing numbers of openings per burst was probably due to decreased missed openings in bursts with multiple long openings (see Discussion). The relative areas of

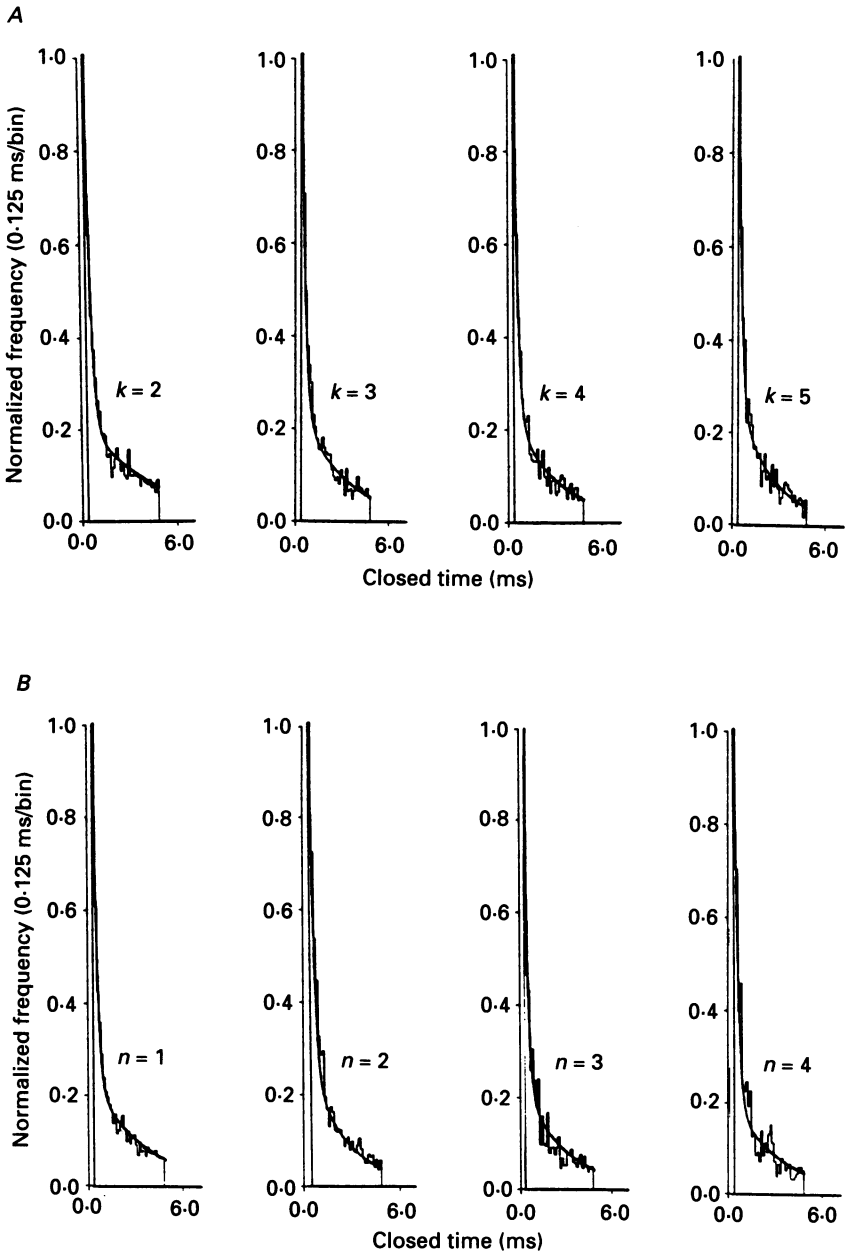

Fig. 8. *A*, normalized frequency distributions of closings within bursts containing two to five openings (2 μM-GABA). Bursts contained two to five openings ($k = 2$ to $k = 5$, respectively). Closings were binned in 0·125 ms bins and displayed over a range of 0·375–5·0 ms. Distributions were fitted with two exponential functions. Histograms contained 2466, 2254, 1941 and 1680 closings for $k = 2$, 3, 4 and 5 opening bursts, respectively. *B*, normalized frequency distributions of the first to fourth closings in all bursts (GABA, 2 μM). The first ($n = 1$), second ($n = 2$), third ($n = 3$) and fourth ($n = 4$) closings of all bursts were binned in 0·125 ms bins and displayed over a range of 0·375–5·0 ms. Distributions were fitted with two exponential functions. Histograms contained 5420, 2954, 1827 and 1180 closings for $n = 1$, 2, 3 and 4, respectively.

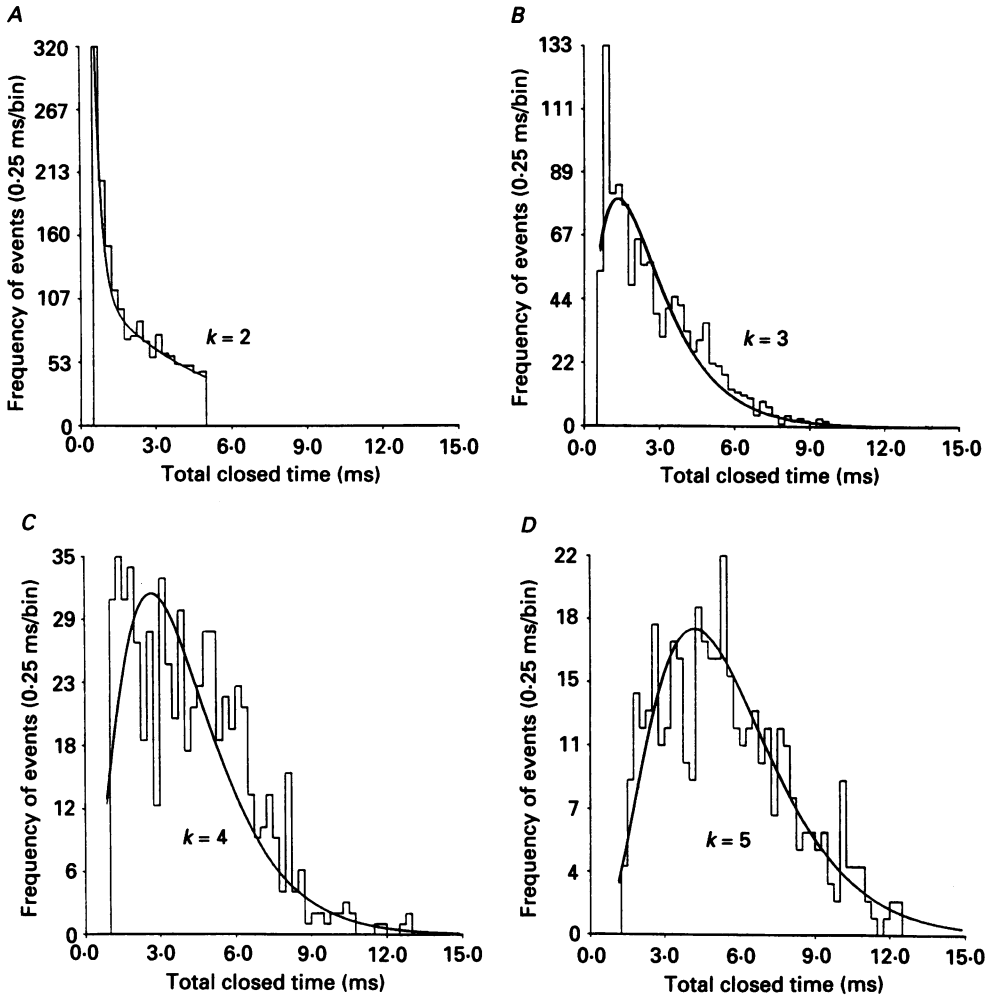

Fig. 9. Distribution of total closed time within bursts containing two to five openings (2 μM-GABA). Total closed times were binned in 0·25 ms bins and displayed over a range of 0·5–15·0 ms. Two opening bursts ($k = 2$) had only one closure and the total closed time was fitted with two exponential functions (*A*). The total closed time within three ($k = 3$; *B*, four ($k = 4$; *C* and five ($k = 5$; *D*) opening bursts were fitted with a single gamma distribution. Histograms contained 2466, 1127, 647 and 420 bursts for $k = 2$, 3, 4 and 5 opening bursts.

the two components also did not vary significantly and were $0{\cdot}54 \pm 0{\cdot}05$ and $0{\cdot}46 \pm 0{\cdot}05$, respectively. Similar results were found for 0·5 and 1 μM-GABA (not illustrated).

Closed time frequency histograms for 2 μM-GABA did not vary with closing position within bursts (Fig. 8*B*). Frequency histograms for the first to fourth intraburst closures were best fitted with two exponential functions. The time constants of the functions did not vary significantly with first to fourth closure position within bursts and averaged $0{\cdot}20 \pm 0{\cdot}01$ and $3{\cdot}1 \pm 0{\cdot}4$ ms. The relative areas

also did not vary with closure position and were $0{\cdot}57 \pm 0{\cdot}03$ and $0{\cdot}43 \pm 0{\cdot}03$, respectively. Similar results were found for 0·5 and 1 μM-GABA (not illustrated).

Similar to the analysis of total open time per burst, total closed time per burst for bursts with two to four closures were fitted with a sum of gamma distributions. Bursts with one closure (two opening bursts) were fitted with two exponential functions as described above. The total closed time for two to four closure bursts were best fitted with a single gamma distribution at each concentration (Fig. 9). The time constants of the distributions were concentration-independent. For 2 μM-GABA, the time constants for two to four closure bursts averaged $1{\cdot}34 \pm 0{\cdot}05$ ms.

DISCUSSION

Intraburst open state kinetics

The main conductance state of GABA receptor channels has been shown to open in bursts of one or more openings with mean burst duration and burst frequency increasing as GABA concentration increased from 0·5 to 5 μM (Macdonald *et al.* 1989). In the present study, we examined the kinetic structure of these bursts. It was found that the mean number of openings per burst increased with concentration, suggesting a two sequential agonist binding reaction (Colquhoun & Hawkes, 1981). The frequency histogram of the number of openings per burst was fitted to three similar geometric functions at each concentration of GABA, indicating that the GABA receptor channel opened in bursts with a mean of about one, two and four openings per burst at all three concentrations of GABA. The relative proportion of one opening bursts decreased with increasing GABA concentration while the relative proportion of the two and four opening bursts increased with increasing GABA concentration. The basis for the concentration-dependent increase in mean number of openings per burst was due to an increase in the relative frequency of occurrence of bursts with multiple mean openings per burst.

We previously suggested the presence of three open states (O_1, O_2 and O_3) for the GABA receptor channel and that the proportion of openings into the O_2 and O_3 states increased while those into the O_1 state decreased with concentration (Macdonald *et al.* 1989). In the present study, we evaluated the distribution of openings in one to five opening bursts, openings at any position of two to five opening bursts, the first to the fourth opening of any burst and the total open time per burst. The results confirmed the presence of the three open states O_1, O_2 and O_3.

Comparison of geometric, intraburst open time and total open time analyses

The data in this study are consistent with the presence of three open states (O_1, O_2 and O_3) which open in bursts with three different mean numbers of openings. As GABA concentration increased, the relative proportion of O_1 openings and singly opening bursts declined, and the relative proportion of O_2 and O_3 openings and multiply opening bursts increased. These data suggest that O_1 openings occur with a mean of 1·1 openings per burst and that O_1 openings originate from a closed state whose binding sites are not all occupied by agonist. In addition, these data suggest that O_2 and O_3 openings occur with a mean of about two and four openings per burst

and originate from fully liganded closed states. These conclusions are consistent with kinetic scheme (3). The finding that the total open time distributions for $k = 1$–5 opening bursts could be fitted by the sum of gamma distributions and that their time constants and areas were not different than those found for the open time distribution for $k = 1$–5 opening bursts suggests that each open state produces a burst of openings primarily by opening several times in succession. Each O_1, O_2 or O_3 state was likely to open once or several times, oscillating between itself and at least one closed state. For example, a series of openings such as $O_3 \rightarrow$ closed state $\rightarrow O_3 \rightarrow$ closed state $\rightarrow O_3$ would be a burst composed of three consecutive O_3 state openings. These data are consistent with the assumption of three open states that open in bursts by closing and reopening to the same open state a characteristic mean number of times.

Since the open time constants for the three open states and their average number of openings per burst did not change with GABA concentration, it is likely that the rate constants for transitions among open states were small. However, it is possible that some transitions between open states occur. With small time bins (125 μs), open time frequency histograms often contain fewer than expected openings in shortest time bins. The presence of a peak in the open time probability distribution well beyond the system dead time, suggests the presence of a minor irreversible reaction step, possibly between open states (Gration, Lambert, Ramsey, Rand & Usherwood, 1982). In general, however, the properties of the open states presented in this study are consistent with those predicted by kinetic scheme (3).

Intraburst closed state kinetics

Since two exponential functions were required to fit the intraburst closed time distributions, it is likely that there were at least two intraburst closed states. Kinetic scheme (2) predicted that three intraburst closed states were present. It is possible that more than two intraburst closed states were present but that several of them had similar dwell times, and therefore, they could not be identified as separate closed states. This alternative was unlikely since the relative proportion of the two closed states did not change with GABA concentration or with position within the burst (as would be predicted from scheme (3)). Since bursts were probably composed of repeated openings of each open state, scheme (3) would predict that the closed states connected to each open state would be the primary closed state in a burst of that open state. This would result in correlated closings of each closed state, and total closed time distributions should be fitted by two gamma distributions. Since the total closed time distributions were fitted by only one gamma distribution with a time constant intermediate in value between the two intraburst closed time constants, it is unlikely that each closed state within a burst repeatedly oscillates to an open state and back to itself. Furthermore, the finding that the two intraburst closed state mean dwell times and relative proportions were not GABA concentration dependent and that the mean intraburst closed time and time constant for the single gamma distribution fits of the $k = 1$–5 openings bursts were similar suggested that the intraburst closed states originated with similar probability from each of the open states and had the same closing rates independent of which open state preceded the intraburst closure.

Basis for the intraburst closures

The basis for fast intraburst closures of neurotransmitter receptor channels is unclear (Colquhoun & Sakmann, 1985). It has generally been concluded that the closures represent entry into closed states from open states and that the closed states are ligand-bound states (see scheme (2)). This might be called agonist-dependent channel gating. However, other alternative mechanisms are possible which might be independent of agonist-dependent channel gating (Colquhoun & Sakmann, 1985).

The intraburst closed states could represent open channel blocked states. The blocking compound could be the agonist molecules, ions or unknown membrane-bound constituents. Alternatively, the closed states could be located distal to the open states. For example, each open state might enter one or more rapidly reversible desensitized states, or while the channel is open, random thermal motion of portions of the channel proteins might produce transient and reversible occlusions of the channel (Läuger, 1988).

Since the two intraburst closed time constants were independent of the number of openings contained in a burst and independent of concentration, the opening rates from the brief intraburst closed states within all of the bursts were similar. This suggests that these intraburst closed states may represent blocked states of the channel or closed states of the channel which occur independent of agonist-dependent channel gating.

The possibility that the brief closed states could be due to channel block produced by agonist (Sine & Steinbach, 1984; Ogden & Colquhoun, 1985) is unlikely since intraburst open time constants did not decrease and closures per burst did not increase when GABA concentration was increased. Alternatively, the brief closed states could be due to open channel block by ions. In our recording solutions, potential blocking anions included chloride, hydroxide and HEPES anions. Recently, it has been reported that the anionic buffer HEPES, but not cationic buffers such as Tris, may block chloride channels (Yamamoto & Suzuki, 1987). Our preliminary studies evaluating the possibility that HEPES may be the source of the intraburst closed times have been inconclusive. However, in experiments using Tris as an intrapipette solution buffer, bursting currents were still observed. Detailed analysis of these currents has not yet been performed.

While the basis for the closed short states is uncertain, the results are consistent with all three open states closing to similar intraburst closed states. Reaction scheme (3) thus inadequately models this behaviour of the GABA receptor main conductance channel. To account for the behaviour of the intraburst closed states, we propose a new kinetic scheme (scheme (4)) which has been modified to account for the intraburst closed time kinetics.

In scheme (4), n represents the number of agonist molecules bound to the receptor ($n = 1, 2$), and O_i represents the ith open state ($i = 1, 2, 3$). The relationship of openings with interburst closings is shown in scheme (4a), and the relationship of openings with intraburst closings is shown in scheme (4b). In this kinetic scheme, bursts are due to repeated agonist-independent closures into the C_i' or C_i'' closed (or blocked) states from any of the three open states (scheme (4b)). In this scheme we assume that all intraburst closures are to a similar closed state regardless of the type

of opening. This need not be the case, however, since subtle differences in the intraburst closed states would be difficult to detect using the present techniques. The closing (or blocking) rates into the two intraburst closed states are likely to be similar since the relative proportions of intraburst closed states were almost equal (0·55 and 0·45). However, they have unequal re-opening (or unblocking) rates since the mean intraburst closed times were 0·19 and 3·1 ms. With this scheme, intraburst closed time distributions would be best fitted with two exponential functions. However, since the two intraburst closed states are distal to the open states, there would be random occurrence of the states and the best gamma distribution fit of the total intraburst closed time distribution would require only a single gamma distribution. Also, the intraburst closed time constants would be concentration-independent because they are distal to agonist binding. The intraburst closed time distribution would not change with increasing numbers of openings per burst because all intraburst closings are to the same or very similar two closed states.

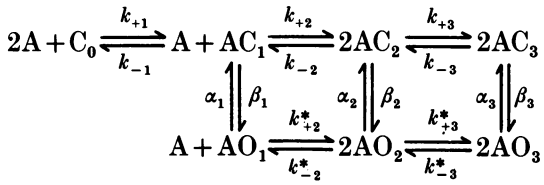

Scheme (4*a*)

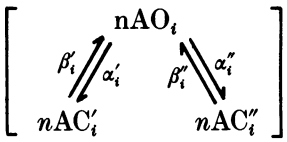

Scheme (4*b*)

Intraburst rate constants

Assuming that the rate constants between open states are minimal and therefore can be disregarded, equations for the effective intraburst rate constants can be obtained from eqns (4–6). These are the rate constants that would be determined based on curve fits of the experimentally obtained frequency histograms without correction for missed events.

$$\tau'_{ci} = (\beta'_i)^{-1} \quad \text{and} \quad \tau''_{ci} = (\beta''_i)^{-1}, \qquad (4a \text{ and } 4b)$$

$$\tau_{oi} = (\alpha_i + \alpha'_i + \alpha''_i)^{-1}, \qquad (5)$$

$$CB_i = (\alpha'_i + \alpha''_i)/\alpha_i. \qquad (6)$$

In eqns (4–6), τ'_{ci} and τ''_{ci} are the two mean intraburst closed times (0·19 and 3·1 ms), τ_{oi} is the mean intraburst open time of the ith open state (0·6, 2·9 and 8·7 ms) and CB_i is the mean number of closings in bursts of the ith open state (0·1, 0·9 and 2·6). From these equations, the effective intraburst rate constants can be calculated using eqns (7–9).

$$\beta_i' = (\tau_{ci}')^{-1} \quad \text{and} \quad \beta_i'' = (\tau_{ci}'')^{-1}, \qquad (7a \text{ and } 7b)$$

$$\alpha_i = (\tau_{oi}\,\mathrm{OB}_i)^{-1}, \qquad (8)$$

$$\alpha_i' = a_i\alpha_i\,\mathrm{CB}_i/(1+a_i) \quad \text{and} \quad \alpha_i'' = \alpha_i\,\mathrm{CB}_i/(1+a_i). \qquad (9a \text{ and } 9b)$$

In eqns (7–9), OB_i are the mean number of openings in bursts of the ith open state ($\mathrm{OB}_i = \mathrm{CB}_1 + 1$), and a_i is the ratio of the relative frequency of occurrence of C_i' and C_i'' (1·22). From eqns (7*a* and 7*b*), the opening rates β_i' and β_i'' are 5263 and 323 s^{-1}, respectively. From eqn (8), α_1, α_2 and α_3 are 1515, 181 and 32 s^{-1}. From eqns (9*a* and 9*b*), α_1' and α_1'' are 83 and 68 s^{-1}, α_2' and α_2'' are 90 and 73 s^{-1} and α_3' and α_3'' are 47 and 37 s^{-1}, respectively.

Preliminary Q-matrix simulation for the GABA receptor channel main conductance state

The values of effective rate constants calculated above were used to determine the intraburst properties predicted by kinetic scheme (4) using the Q-matrix approach of Colquhoun & Hawkes (1977, 1981, 1982). Since the data were obtained from multichannel patches, no attempt was made to fit accurately interburst closed time distributions or to determine accurately the transition probabilities between interburst closed states. Patches were selected which had rare multiple openings. We estimate that these patches had an average of 2·5 channels per patch. At 2 μM the GABA receptor main state was open 4·7 % of the time (equilibrium occupancy of about 1·9 % per channel) and 11·4 openings per second (about 4·5 openings per second per channel) were recorded. After correction for missed openings with durations less than the system dead time, extraburst rate constants were selected to match the above equilibrium occupancy and opening frequency. The following extraburst effective rate constants were used in the simulations: k_{+1} ($2{\cdot}5 \times 10^6$ M^{-1} s^{-1}), k_{-1} (12·5 s^{-1}), k_{+2} ($2{\cdot}5 \times 10^6$ M^{-1} s^{-1}), k_{-2} (12·5 s^{-1}), k_{+3} (30·0 s^{-1}), k_{-3} (125·0 s^{-1}), β_1 (2·77 s^{-1}), β_2 (12·5 s^{-1}) and β_3 (17·5 s^{-1}). In this simulation, the affinity of the GABA receptor for each binding site was assumed to be equivalent and equal to 5 μM.

With these effective rate constants, the mean open time would be 4·4 ms (4·3 ms was the measured mean open time corrected for missed openings), the mean number of openings per burst would be 2·0 (1·9 was the measured mean number of openings per burst), the mean burst duration would be 10·7 ms (10·1 was the measured mean burst duration corrected for missed openings) and the mean intraburst closed time would be 1·4 ms (1·4 ms was the measured mean intraburst closed time corrected for missed closures). Thus the kinetic scheme accurately predicts mean burst parameters. A more stringent test, however, is to compare the probability density functions predicted by the scheme with the frequency histograms obtained experimentally. Kinetic scheme (4) predicts that the open duration probability density function would consist of three components (Table 5) whose time constants and relative areas are close to those found experimentally. Similarly, scheme (4) predicts that the geometric distribution of openings per burst would be composed of three components whose mean number of openings per burst are similar to those found experimentally (Table 5). The theoretical and experimental geometric functions differ somewhat,

TABLE 5. Comparison of components for open time, burst duration and openings per burst histograms with Q-matrix solutions

Component	1	2	3	4
Open duration τ (area)	0·59 (0·17)	2·9 (0·54)	8·9 (0·30)	—
Open duration Q	0·60 (0·16)	2·9 (0·53)	8·7 (0·31)	—
Burst duration τ (area)	0·54 (0·26)	2·3 (0·17)	8·0 (0·33)	30·7 (0·22)
Burst duration Q	0·63 (0·28)	2·3 (0·08)	8·1 (0·45)	35·0 (0·18)
Openings/burst μ (area)	1·1 (0·50)	2·2 (0·35)	3·9 (0·15)	—
Openings/burst Q	1·1 (0·30)	2·0 (0·52)	3·6 (0·18)	—

The measured components ($i = 1, 2, 3, 4$) for open time, burst duration and openings per burst obtained for 2 μM-GABA were compared to those obtained by a Q-matrix simulation of scheme (4) (see text). Open duration and burst duration time constants (τ_i) are in milliseconds with the relative area in parentheses (eqn (2)). Openings per burst components are means (μ_i) with the relative area in parentheses (eqn (1)). Components designated by dashes indicate that those components were not calculated for scheme (4).

TABLE 6. All openings in a burst with k openings, components of exponential functions and Q-matrix solution for 2 μM + GABA

	$k = 1$	$k = 2$	$k = 3$	$k = 4$	$k = 5$
τ_1	0·6	0·6	0·6	—	—
τ_2	2·9	2·9	2·9	2·9	2·9
τ_3	8·7	8·7	8·7	8·7	8·7
a_1	0·46	0·10	0·02	—	—
a_2	0·45	0·70	0·70	0·64	0·55
a_3	0·09	0·20	0·28	0·36	0·45

The open time probability density functions for 2 μM-GABA were obtained by Q-matrix simulation of scheme (4) (see text). Open duration time constants (τ_i) for open components $i = 1$, 2, 3 are presented with the corresponding relative area (a_i). Time constants are in milliseconds. Components designated by dashes indicate that those components contributed less than 1 % of the total area.

however, in the estimate of the relative proportion of the bursts with about 1·1 and 2·0 openings per burst. This may be due to the absence of any correction of the openings per burst histogram. Since there were missed brief events, it is likely that a proportion of bursts will have too few openings per burst, and therefore, there will be a shift of the experimentally obtained openings per burst histogram towards fewer openings. Consistent with this interpretation, the openings per burst histograms for 0·5, 1·0 and 5·0 μM were all fitted with three geometric functions with the same mean numbers of openings per burst but with an excess of bursts with few openings (data not presented). The burst duration histogram was fitted by three exponential functions with a significant χ^2 value. Scheme (4) predicts that the burst duration probability density function should consist of nine exponential functions. However, 98·2 % of the probability density function can be accounted for by four components. Therefore, the burst duration histogram was fitted by four exponential components, and the experimental and theoretical results were compared (Table 5). There was good agreement between the time constants and the relative areas of the four components predicted by scheme (4) and those obtained experimentally. In addition, the open time distributions as a function of GABA concentration and the intraburst

closed time distributions for bursts of two to four openings were similar to those predicted by the Q-matrix simulation (numerical values of the Q-matrix solutions not presented).

Using the above rate constants, kinetic scheme (4) predicts that the distribution of open times would vary with the number of openings in a burst (Table 6). The Q-matrix simulation predicts that the relative proportion of short (0·6 ms) openings would be maximal in one event bursts and be undetectable in bursts with three or more openings. The relative proportion of longer openings (2·9 ms) would increase with increasing numbers of openings per burst, reaching a maximum in two and three opening bursts, and would then decline. The relative proportion of the longest (8·7 ms) openings would be smallest in one event bursts but would increase with increasing numbers of openings per burst. The distributions predicted by the Q-matrix simulation (Table 6) were similar to those obtained experimentally (Table 2).

In summary, the Q-matrix simulation of scheme (4) generates intraburst distributions which are quite similar to those obtained experimentally and lends support to the suggestion that scheme (4) may be an acceptable kinetic scheme for the gating of the $GABA_A$ receptor main conductance state.

Correction of effective rate constants for missed events

Due to the limited frequency response and low-pass filtering used in these experiments, brief openings and closings with durations less than the system dead time (about 170 μs) were missed (Sachs, Neil & Barkakati, 1982; Colquhoun & Sigworth, 1983; Neher, 1983). As a result the time constants obtained experimentally are probably too long, and thus, the effective rate constants obtained using the Q-matrix simulation will differ from the true rate constants (Blatz & Magleby, 1986*a*). However, once a gating scheme has been determined, there are methods to correct for missed events (Sachs *et al.* 1982; Colquhoun & Sigworth, 1983; Neher, 1983; Roux & Sauve, 1985; Blatz & Magleby, 1986*a*). We have used the method of Blatz & Magleby (1986*a*) to determine the effect of missed events on the effective intraburst rate constants determined for scheme (4) using the Q-matrix simulation.

The general approach for correcting for missed events is to examine the possible transition pathways that occur from each state and then to determine which transitions are likely to be missed with high frequency. We have used this method to correct for missed intraburst events. We assume that interburst closures are rarely missed while intraburst closures and openings are missed with relatively higher frequency. We have used the general model shown in scheme (5) to calculate the effect of missed intraburst events (see Appendix).

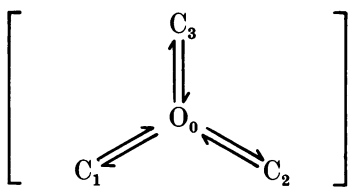

Scheme (5)

To correct for missed events, it was assumed (1) that the opening (β'_i and β_i) rates from the intraburst closures to the three open states were similar, (2) that the best

assessment of intraburst effective closed time constants were obtained from closures in bursts with more than three openings since those closures were adjacent to longer duration openings, (3) that the effective open time constants were 0·6, 2·9 and 8·7 ms, (4) that the effective intraburst closed time constants were 0·19 and 3·1 ms and (5) that the effective openings per burst were 1·07, 1·9 and 3·6. Based on these assumptions, the true open time constants were 0·55, 2·0 and 5·1 ms, the true intraburst closed time constants were 0·18 and 3·0 ms and the true openings per burst were 1·2, 2·8 and 6·0 openings per burst. The true intraburst rate constants were as follows: α_1, α_2 and α_3 were 1530, 184 and 29·7 s^{-1}, α_1' and α_1'' were 223 and 69·0 s^{-1}, α_2' and α_2'' were 241 and 74·4 s^{-1}, α_3' and α_3'' were 126 and 38·7 s^{-1}, and β_1' and β_1'' were 5500 and 332 s^{-1}, respectively.

Conclusions

These data are consistent with kinetic scheme (4). However, the ability to model the properties of the main conductance state of the GABA receptor by a single kinetic scheme does not prove that the kinetic scheme is correct. Other schemes may also predict the kinetic behaviour of the channel (Blatz & Magleby, 1986*b*). Furthermore, this scheme does not include desensitization states, and therefore, is incomplete. None the less, this kinetic scheme will be useful in the study of the effect of a wider range of GABA concentrations and of the effect of allosteric regulators of the GABA receptor such as barbiturates, benzodiazepines and picrotoxin-like drugs.

APPENDIX

Due to the limited system frequency response of our recording system, brief openings and closings were missed. The following equations were used to determine the effect of missed events on intraburst time constants and events per burst. For this analysis, D is the system dead time, L_i is the true mean lifetime of state i, τ_{obs0} is the observed time constant of decay for state 0, F_{missi} is the fraction of missed state i events, F_{capi} is the fraction of captured state i events and T_{missi} is the mean duration of missed state i events. By analogy to eqn (16) of Blatz & Magleby (1986*a*), τ_{obs0} can be determined using eqn (A 1). Each open state was corrected independently by inserting the appropriate rate constants into scheme (5).

$$\tau_{obs0} = (L_0 + \Sigma a_i F_{missi} \Sigma a_i T_{missi})/(\Sigma a_i F_{capi}), \quad \text{(A 1)}$$

where $i = 1$–3 and a_i are the relative areas of the closed states ($a_1 + a_2 + a_3 = 1$). Also,

$$F_{missi} = 1 - \exp(-D/L_i), \quad \text{(A 2)}$$

$$F_{capi} = \exp(-D/L_i), \quad \text{(A 3)}$$

and

$$T_{missi} = (L_i - (L_i + D)\exp(-D/L_i))/F_{missi}. \quad \text{(A 4)}$$

The effective rate constant from the ith closed state to the open state 0 (k_{i0eff}) can be determined using eqn (A 5).

$$k_{i0eff} = F_{capo}/(L_i + F_{misso} T_{misso}). \quad \text{(A 5)}$$

The effective rate constant constant from the open state to the ith closed state ($k_{0i\text{eff}}$) can be determined using eqn (A 6).

$$k_{0i\text{eff}} = a_i F_{\text{cap}i}/(L_0 + \Sigma a_i F_{\text{miss}i} T_{\text{miss}i}), \quad \text{(A 6)}$$

where the sum in eqn (A 6) is $i = 1$–3.

The authors wish to thank Ms Nancy Fox for technical assistance in the preparation and maintenance of cell cultures and in the preparation of the figures, Dr Barry Pallotta for providing a version of his Q-matrix program and Dr Karl Magleby for helpful discussions.

REFERENCES

BLATZ, A. L. & MAGLEBY, K. L. (1986*a*). Correcting single channel data for missed events. *Biophysical Journal* **49**, 967–980.

BLATZ, A. L. & MAGLEBY, K. L. (1986*b*). Quantitative description of three modes of activity of fast chloride channels from rat skeletal muscle. *Journal of Physiology* **378**, 141–174.

BORMANN, J. (1988). Electrophysiology of $GABA_A$ and $GABA_B$ receptor subtypes. *Trends in Neurosciences* **11**, 112–116.

BORMANN, J. & CLAPHAM, D. E. (1985). γ-Aminobutyric acid receptor channels in adrenal chromaffin cells: a patch-clamp study. *Proceedings of the National Academy of Sciences of the USA* **82**, 2168–2172.

BORMANN, J., HAMILL, O. P. & SAKMANN, B. (1987). Mechanism of anion permeation through channels gated by glycine and γ-aminobutyric acid in mouse cultured spinal neurones. *Journal of Physiology* **385**, 243–286.

COLQUHOUN, D. (1973). The relation between classical and cooperative models for drug action. In *Drug Receptors*, ed. RANG, H. D., pp. 149–182. University Press, Baltimore, MD, USA.

COLQUHOUN, D. & HAWKES, A. G. (1977). Relaxation and fluctuations of membrane currents that flow through drug-operated channels. *Proceedings of the Royal Society* B **199**, 231–262.

COLQUHOUN, D. & HAWKES, A. G. (1981). On the stochastic properties of single ion channels. *Proceedings of the Royal Society* B **211**, 205–235.

COLQUHOUN, D. & HAWKES, A. G. (1982). On the stochastic properties of bursts of single ion channel openings and clusters of bursts. *Philosophical Transactions of the Royal Society* B **300**, 1–59.

COLQUHOUN, D. & HAWKES, A. G. (1983). The principles of the stochastic interpretation of ion-channel mechanisms. In *Single-Channel Recording*, ed. SAKMANN, B. & NEHER, E., pp. 135–175. Plenum Press, New York.

COLQUHOUN, D. & OGDEN, D. C. (1988). Activation of ion channels in the frog end-plate by high concentrations of acetylcholine. *Journal of Physiology* **395**, 131–159.

COLQUHOUN, D. & SAKMANN, B. (1985). Fast events in single-channel currents activated by acetylcholine and its analogues at the frog muscle end-plate. *Journal of Physiology* **369**, 501–557.

COLQUHOUN, D. & SIGWORTH, F. J. (1983). Fitting and statistical analysis of single-channel records. In *Single-Channel Recording*, ed. SAKMANN, B. & NEHER, E., pp. 191–263. Plenum Press, New York.

DEL CASTILLO, J. & KATZ, B. (1957). Interaction at end-plate receptors between different choline derivatives. *Proceedings of the Royal Society* B **146**, 369–381.

DIONNE, V. E. & LIEBOWITZ, M. D. (1982). Acetylcholine receptor kinetics: a description from single-channel currents at snake neuromuscular junctions. *Biophysical Journal* **39**, 253–261.

DIONNE, V. E., STEINBACH, J. H. & STEVENS, C. F. (1978). An analysis of the dose–response relationship at voltage-clamped neuromuscular junctions. *Journal of Physiology* **281**, 421–444.

DREYER, F., PEPER, K. & STERZ, R. (1978). Determination of dose–response curves by quantitative ionophoresis at the frog neuromuscular junction. *Journal of Physiology* **281**, 395–419.

DUDEL, J. & FRANKE, C. (1987). Single glutamate-gated synaptic channels at the crayfish neuromuscular junction II: Dependence of channel open time on glutamate concentration. *Pflügers Archiv* **408**, 307–314.

GRATION, K. A. F., LAMBERT, J. J., RAMSEY, R. L., RAND, R. P. & USHERWOOD, P. N. R. (1982). Closure of membrane channels gated by glutamate receptors may be a two-step process. *Nature* **295**, 599–601.

HAMILL, O. P., BORMANN, J. & SAKMANN, B. (1983). Activation of multiple-conductance state chloride channels in spinal neurones by glycine and GABA. *Nature* **305**, 805–808.

HAMILL, O. P., MARTY, A., NEHER, E., SAKMANN, B. & SIGWORTH, F. J. (1981). Improved patch-clamp techniques for high-resolution current recording from cells and cell-free membrane patches. *Pflügers Archiv* **391**, 85–100.

HESTRIN, S., KORENBROT, J. I. & MARICQ, A. V. (1987). Kinetics of activation of acetylcholine receptors in a mouse muscle cell line under a range of acetylcholine concentrations. *Biophysical Journal* **51**, 449–455.

HOWE, J. R., COLQUHOUN, D. & CULL-CANDY, S. G. (1988). On the kinetics of large-conductance glutamate-receptor ion channels in rat cerebellar granule neurons. *Proceedings of the Royal Society* B **233**, 407–422.

JACKSON, M. B. (1988). Dependence of acetylcholine receptor channel kinetics on agonist concentration in cultured mouse muscle fibres. *Journal of Physiology* **397**, 555–583.

KARLIN, A. (1967). On the application of 'a plausible model' of allosteric proteins to the receptor for acetylcholine. *Journal of Theoretical Biology* **16**, 306–320.

KERRY, C. J., KITS, K. S., RAMSEY, R. L., SANSOM, M. S. & USHERWOOD, P. N. R. (1987). Single channel kinetics of a glutamate receptor. *Biophysical Journal* **51**, 137–144.

KERRY, C. J., RAMSEY, R. L., SANSOM, M. S. P. & USHERWOOD, P. N. R. (1988). Glutamate receptor kinetics: the effect of concentration. *Biophysical Journal* **53**, 39–52.

LABARCA, P., RICE, J. A., FREDKIN, D. R. & MONTAL, M. (1985). Kinetic analysis of channel gating: application to the cholinergic receptor channel and the chloride channel from *Torpedo californica*. *Biophysical Journal* **47**, 469–478.

LÄUGER, P. (1988). Internal motions in proteins and gating kinetics of ionic channels. *Biophysical Journal* **53**, 877–884.

MACDONALD, R. L., ROGERS, C. J. & TWYMAN, R. E. (1989). Kinetic properties of the $GABA_A$ receptor main conductance state of mouse spinal cord neurones in culture. *Journal of Physiology* **410**, 479–499.

MCMANUS, O. B., BLATZ, A. L. & MAGLEBY, K. L. (1987). Sampling, log binning, fitting and plotting durations of open and shut intervals from single channels and the effects of noise. *Pflügers Archiv* **410**, 530–553.

MARTIN, R. J. (1985). γ-Aminobutyric acid- and piperazine-activated single-channel currents from *Ascaris suum* body muscle. *British Journal of Pharmacology* **84**, 445–461.

MONOD, J., WYMAN, J. & CHANGEUX, J. P. (1965). On the nature of allosteric transitions: a plausible model. *Journal of Molecular Biology* **12**, 88–118.

NEHER, E. (1983). The charge carried by single-channel currents of rat cultured muscle cells in the presence of local anaesthetics. *Journal of Physiology* **339**, 663–678.

OGDEN, D. D. & COLQUHOUN, D. (1985). Ion channel block by acetylcholine, carbachol and suberyldicholine at the neuromuscular junction. *Proceedings of the Royal Society* B **225**, 329–355.

PAPKE, R. L., MILLHAUSER, G., LIEBERMAN, Z. & OSWALD, R. E. (1988). Relationships of agonist properties to the single channel kinetics of nicotinic acetylcholine receptors. *Biophysical Journal* **53**, 1–10.

RANSOM, B. R., NEALE, E., HENKART, M., BULLOCK, P. N. & NELSON, P. G. (1977). Mouse spinal cord in cell culture. I. Morphology and intrinsic neuronal electrophysiological properties. *Journal of Neurophysiology* **40**, 1132–1150.

ROUX, B. & SAUVE, R. (1985). A general solution to the time interval omission problem applied to single channel analysis. *Biophysical Journal* **48**, 149–158.

SACHS, F., NEIL, C. & BARKAKATI, N. (1982). The automated analysis of data from single ionic channels. *Pflügers Archiv* **395**, 331–340.

SAKMANN, B., HAMILL, O. P. & BORMANN, J. (1983). Patch-clamp measurements of elementary chloride currents activated by the putative inhibitory transmitters GABA and glycine in mammalian spinal neurons. *Journal of Neural Transmission Supplementum* **18**, 83–95.

SINE, S. M. & STEINBACH, J. H. (1984). Agonists block currents through acetylcholine receptor channels. *Biophysical Journal* **46**, 277–283.

SINE, S. M. & STEINBACH, J. H. (1986). Activation of acetylcholine receptors on clonal mammalian BC3H-1 cells by low concentrations of agonist. *Journal of Physiology* **373**, 129–162.

WEISS, D. S., BARNES, E. M. & HABLITZ, J. J. (1988). Whole-cell and single-channel recordings of GABA-gated currents in cultured chick cerebral neurons. *Journal of Neurophysiology* **59**, 495–513.

YAMAMOTO, D. & SUZUKI, N. (1987). Blockage of chloride channels by HEPES buffer. *Proceedings of the Royal Society* B **230**, 93–100.